Structure, Conformational Equilibrium, and Proton Affinity of Calix[4]arene by Density Functional Theory

R. J. Bernardino[†] and B. J. Costa Cabral*[,†,‡]

Centro de Física da Matéria Condensada da Universidade de Lisboa, Avenida Professor Gama Pinto 2, 1649-015 Lisboa, Portugal, and Departamento de Química e Bioquímica, Faculdade de Ciências da Universidade de Lisboa, Rua Ernesto Vasconcelos, Edifício C1, 1700 Lisboa, Portugal

Received: April 14, 1999; In Final Form: July 20, 1999

Density functional theory results for the structure and conformational equilibrium of four calix[4]arene conformers are reported. The results are compared with experiment, force field, and semiempirical molecular orbital calculations. The energy difference between the two most stable conformers of calix[4]arene (cone and partial-cone) is 10 kcal mol^{-1} at the BLYP/6-31G** level with the geometries optimized at BLYP/6-31G*. For the most stable conformer, results for the protonated structure are also reported. Electrostatic potential surfaces for the cone calix[4]arene and the corresponding tetra-O−H-depleted structure have been calculated. It is suggested that their representation may be of relevance to understand the known ability of calix[*n*]arene systems to form complexes with charged species in host−guest chemistry.

I. Introduction

Molecular systems having the ability to recognize or selectively interact with other molecules are extremely important in chemistry or biochemistry. One of the most relevant application of these systems is in host−guest chemistry. In this field, recognition is related to selective host−guest receptors and it is strongly dependent on the host−guest intermolecular interactions.

One family of model systems in supramolecular host−guest chemistry is the family of calix[*n*]arenes.[1,2] Calix[*n*]arenes are examples of [1_n]-metacyclophanes composed of phenol and methylene bridged units. One characteristic of the calix[*n*]arene structure is their π-rich cavity, which favors the inclusion of charged guest compounds, which are stabilized by noncovalent binding forces related to cation−π interactions.[3−5] Some recent studies suggested that the investigation of cation−π interactions will contribute to the design of new calix[*n*]arenes-based receptors useful for molecular recognition.[6] In addition, calix[*n*]arenes are highly useful cyclic compounds into which the introduction of functional groups in the lower or in the upper rims can be designed to favor interactions with specific guest systems and lead to the construction of very sophisticated molecular sensors.

The investigation on the structural and energetic basis of selectivity in calix[*n*]arenes and derivatives has been the subject of numerous works.[1,2] One of the best known members of the calix[*n*]arene family is calix[*4*]arene. This system has four stable and relevant conformers:[7] cone, partial-cone, 1,2-alternate, and 1,3-alternate (see Figure 1). Although the reduction to a small number of conformers simplifies considerably the task of modelling calix[4]arene by theoretical calculations, the size of the system makes a full first-principles approach difficult. Consequently, a significant number of works on these systems has been based on force field[8−17] or semiempirical molecular orbital approaches.[8,11,18,19]

In the present work we report density functional results for the structure, conformational equilibrium, and electronic properties of calix[4]arene. Our aim is to provide accurate theoretical information on the conformational equilibrium and electronic properties of this complex molecule by density functional theory calculations. We are also reporting results for the structure of the protonated structure of the cone calix[4]arene conformer. In order to discuss the known ability of calix[4]arene to selectively interact with neutral molecules and charged species, this work also presents data on the electrostatic potential surfaces of calix[4]arene and some related systems. It appears that the electrostatic potential may be of considerable interest to explain some features characterizing calix[*n*]arenes in host−guest chemistry.

II. Computational Details

We have carried out complete geometry optimizations at different theoretical levels using density functional theory. The first set of optimizations has been carried out with the Becke exchange functional only[20] (HFB) and the 6-31G basis set. Optimizations using the Becke representation for the exchange and the Lee, Yang, and Parr correlation functional[22] have been also carried out with the 6-31G and 6-31G* basis set. Further single-point calculations with the 6-31G** basis set and two different representations for the exchange functional (Becke[20] and Becke's three-parameter[21]) are also reported. We have also optimized the structure of the protonated cone conformer at BLYP/6-31G and BLYP/6-31G* level.

The DFT calculations have been carried out with a pruned grid (75,302), having 75 radial shells and 302 angular points per shell (default grid in Gaussian-94). For comparison with other theoretical approaches, results based on AM1,[24] PM3,[25] CHARMM,[26] MM3 and MM^{+} [27] are also reported.

In order to discuss the role played by electrostatic interactions in the complexation of charged species with calix[4]arene, we have calculated the electrostatic potential from BLYP/6-31G* optimizations. We are also providing data on the electrostatic potential for the tetra-O−H-depleted calix[4]arene in which the

* To whom correspondence should be addressed. E-mail: ben@adonis.cii.fc.ul.pt.
† Centro Física da Matéria Condensada.
‡ Departamento de Química e Bioquímica.

10.1021/jp991213h CCC: $18.00
Published on Web 10/23/1999

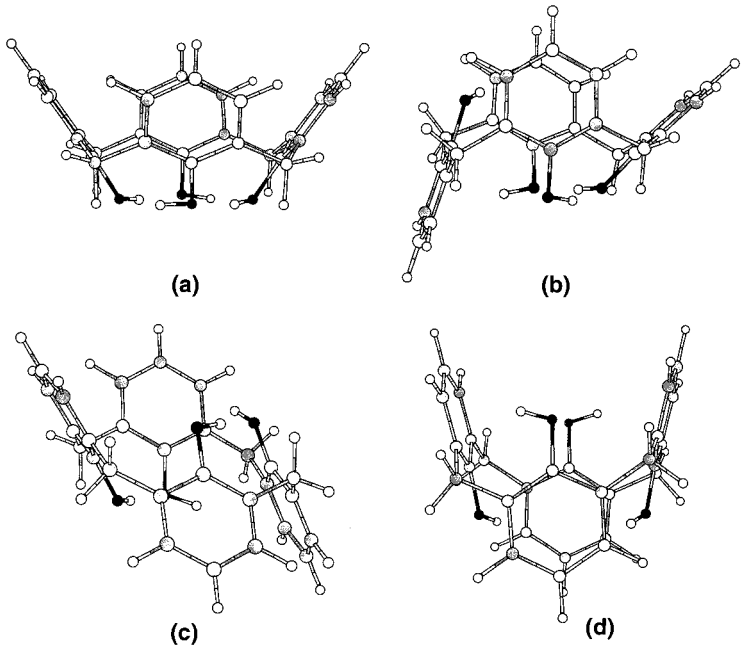

Figure 1. Calix[4]arene conformers. (a) cone, (b) partial-cone, (c) 1,2-alternate, (d) 1,3-alternate.

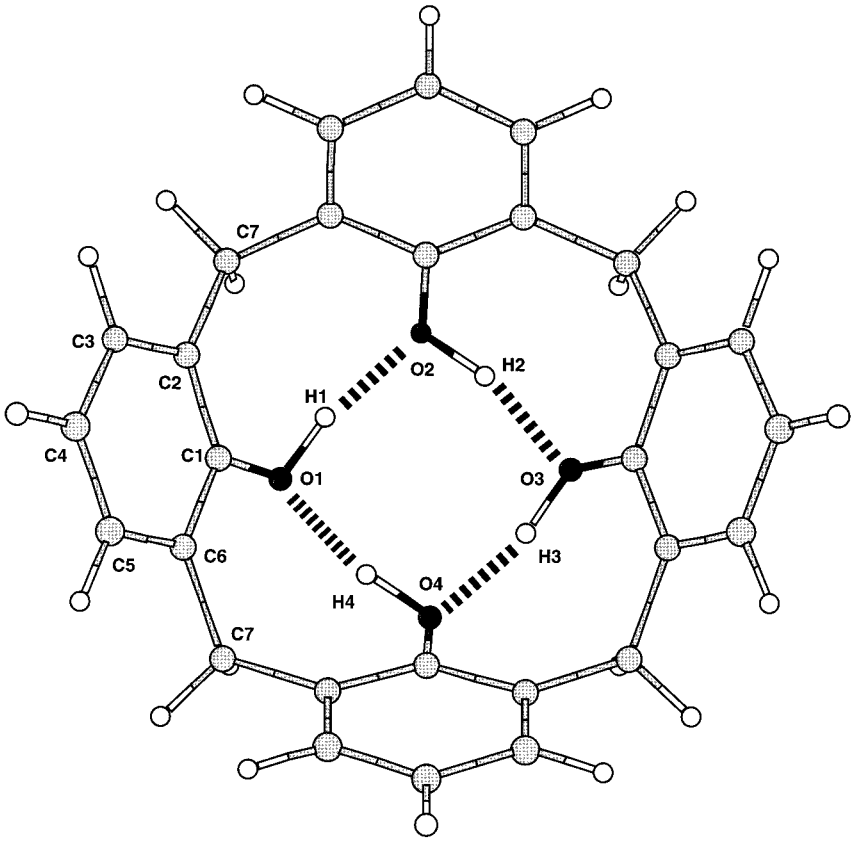

Figure 2. Hydrogen bonding in the calix[4]arene cone conformer. This figure illustrates the formation of a cyclic hydrogen bonded array in the low rim of calix[4]arene.

O−H groups have been replaced by H atoms. The calculations have been performed with the GAUSSIAN-94 program,[23] and the electrostatic potential surfaces have been generated with the Molekel software.[28]

III. Results and Discussion

A. Conformational Equilibrium and Proton Affinity. Figure 1 shows the structure of the four calix[4]arene conformers (cone; partial-cone; 1,2-alternate; 1,3-alternate). Figure 2 illustrates hydrogen bonding in the cone conformer. The total energy of the cone conformer and the energy differences between the others conformers are reported in Table 1. All the calculations predict that the most stable stable conformer is the cone conformer that is stabilized by an array of four hydrogen bonds.

Comparison of HFB/6-31G and BLYP/6-31G results indicate that by using an exchange and correlation functional (BLYP) the cone conformer is significantly stabilized relative to all others

TABLE 1: Total Energies (in au) of the Cone Calix[4]arene Conformer at Different Theoretical Levels[a]

	cone (total)	partial cone (ΔE)	1,2-alternate (ΔE)	1,3-alternate (ΔE)
HFB/6-31G	−1373.860 22	12.1	20.4	20.9
BLYP/6-31G	−1381.508 77	16.0	26.2	27.8
	(−1381.866 96)			
BLYP/6-31G*[b]	−1381.804 62	9.7	17.2	16.3
BLYP/6-31G**[b]	−1381.856 09	10.0	17.4	16.6
BLYP/6-31G*	−1381.810 15	10.7	18.6	18.1
	(−1382.159 52)			
BLYP/6-31G**[c]	−1381.861 09	10.7	18.3	17.7
B3LYP/6-31G**[c]	−1382.360 33	10.5	18.4	17.6
AM1		7.4	10.4	11.5
PM3		7.4	12.4	11.1
CHARMM[d]		9.6	11.8	17.2
MM3(89)[e]		9.9	11.7	18.7
MM3(92)[f]		5.6	6.1	10.6
MM^{+}[b]		7.4	9.3	13.6
experiment[g]		14.9,13.8		

[a] Energy differences (ΔE's in kcal/mol) between the conformers (partial-cone, 1,2-alternate and 1,3-alternate) and the cone conformer. Total energies for the protonated cone are also reported (values in parentheses). [b] Geometry optimized at BLYP/6-31G. [c] Geometry optimized at BLYP/6-31G* [d] From ref 14. [e] From ref 10. [f] From refs 12 and 13. [g] Free energies of activation $\Delta G^{\ddagger}$ in a solvent (chloroform and benzene, respectively) from ref 7.

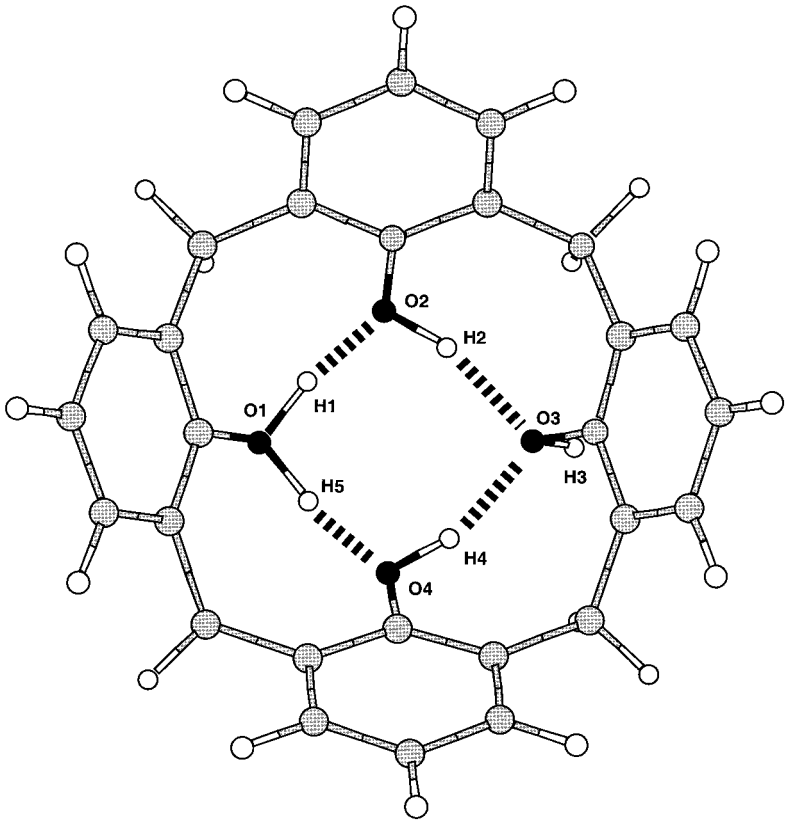

Figure 3. Hydrogen bonding in the protonated calix[4]arene cone conformer. The complexation of calix[4]arene with H^{+} breaks the symmetry of the cone conformer presented in Figure 2.

conformers. Thus, the energy differences between the partial-cone and cone conformer changes from 12.1 kcal mol^{-1} at HFB/6-31G to 16 kcal mol^{-1} at BLYP/6-31G. Introduction of polarization functions on the heavy atoms (6-31G* basis set) reduces the energy difference between the conformers. In addition, at BLYP/6-31G*, the relative stability of conformers 1,2-alternate and 1,3-alternate is inversed when compared to BLYP/6-31G results. However, all density functional calculations predict that the energy difference between these conformers (1,2-alternate and 1,3-alternate) is very low (≈1 kcal mol^{-1}).

Additional single-point calculations with the 6-31G** basis set predict similar values for the conformational energy differences. The energy difference between the two most stable conformers (cone and partial-cone) is 10.7 kcal mol^{-1} at BLYP/6-31G** level with the geometries optimized at BLYP/6-31G*.

Comparison with experimental data is not direct since the available data is from measurements in the liquid phase and solvent effects can be important. Experimental free energies of activation (ΔG's) for conformational inversion of calix[4]arene in different solvents[7] are reported in Table 1.

Table 1 also presents results for the energy differences between the calix[4]arene conformers based on force field and semiempirical molecular orbital calculations. Similar values for the energy differences between the partial cone and cone conformers and also between 1,3-alternate and cone are

TABLE 2: Data for the Structure of Cone Calix[4]arene[a]

	BLYP/6-31G*	AM1	MM3[b]	exptl[c]
		bond distances/Å		
C_1-C_2	1.42	1.41		1.41;1.38
C_1-C_6	1.41	1.41		1.40;1.39
C_2-C_3	1.41	1.40		1.39;1.38
C_2-C_7	1.54	1.50		1.53
C_1-O	1.39	1.38		1.41;1.37
O−O	2.67	2.91	3.05	2.64
		angles/deg		
$C_1-C_2-C_3$	117.6	114.3		117.3
$C_1-C_2-C_7$	122.3	122.7		121.9
$C_1-C_6-C_7$	121.4	121.4		120.8
$C_2-C_7-C_6$	113.9	111.4	112.4	113.0
$C_2-C_1-C_6$	122.1	121.2		121.6
$O_1-C_1-C_2$	120.9	123.0		119.1
$O_1-C_1-C_6$	116.9	115.8		119.3,117.8

[a] We present results from density functional theory (BLYP/6-31G*), semiempirical molecular orbital theory (AM1), force field (MM3), and data from experiment. [b] From ref 10. [c] From ref 29.

predicted by DFT and force field calculations (CHARMM[14] and MM3(89).[10,12,13] However, DFT and semiempirical molecular orbital calculations predict a very low energy difference between 1,2-alternate and 1,3-alternate conformers (less than 1 kcal mol^{-1}), which disagrees significantly with force field results ($\approx$4−6 kcal mol^{-1}). Apparently, this disagreement is not related with significant differences in the structures. This conclusion is supported by single-point calculations at MM^+ level, with geometries optimized at BLYP/6-31G*. From these calculations the energy difference between 1,2-alternate and 1,3-alternate of is $\approx$4 kcal mol^{-1}.

Complexation of calix[*n*]arenes with charged species is extremely important in host-guest chemistry and several works based on force field[6,30] calculations concerning the complexation of alkali metals cations with calix[*n*]arenes have been reported. However, we are not aware of experimental data or theoretical predictions on the proton affinity of calix[4]arene. Figure 3 shows the structure of protonated cone conformer of calix[4]-arene. Total energies for the protonated cone are also reported in Table 1. From the total energies we predict that the proton affinity is 224.8 kcal mol^{-1} at BLYP/6-31G and 219.3 kcal mol^{-1} at BLYP/6-31G*.

B. Structure. Table 2 reports structural information from experiment,[29] density functional (BLYP/6-31G*), semiempirical molecular orbital theory (AM1), and force field calculations (MM3).[10] The experimental data are from the hexagonal phase of the calix[4]arene−acetone clathrate.[29] Although condensed phase structures are not directly comparable to gas phase data, our predictions based on BLYP/6-31G* optimizations are in very good agreement with experiment.[29] We find that the O−O distance calculated by DFT (2.6 Å) is in perfect agreement with experiment. We interpret the agreement between our DFT results and experiment as a strong indication that the present approach (BLYP/6-31G*) is adequate to correctly describe the structure of calix[*n*]arenes. Density functional and AM1 results for the structural parameters of the cone calix[4]arene are in good agreement. One exception is the O−O distance calculated by DFT (2.6 Å) that is much shorter than AM1 (2.9 Å) and MM3-(89) (3.05 Å) predictions.

Table 3 reports data on the structure of the cone and protonated cone (cone-H^+) conformers of calix[4]arene. We have restricted our discussion to the structural parameters related to hydrogen bonding in the lower rim of calix[4]arene. For the cone conformer we can observe a significant reduction of the O−H bonds (H_1-O_2, H_2-O_3, H_3-O_4, H_4-O_1) when we move from HFB/6-31G to BLYP/6-31G. This dependence suggests that electronic correlation effects contributes to significantly reduce the O−H bond lengths. Introduction of polarization functions on the heavy atoms (moving from BLYP/6-31G to BLYP/6-31G*) increases the O−H bonds by 0.1 Å. Valence angles ($O_1-H_1-O_2$, $O_2-H_2-O_3$, $O_3-H_3-O_4$, $O_4-H_4-O_1$) are increased by $\approx$4°.

Protonation breaks the symmetry of the cyclic O−H bond array. In addition, some O−H bonds are clearly increased (H_2-O_3, H_4-O_3) while H_1-O_2 is reduced. Comparison between the different basis sets (6-31G and 6-31G*) shows that some parameters are significantly modified. Thus, H_5-O_4 is 1.39 Å at BLYP/6-31G and 1.46 Å at BLYP/6-31G*. $O_4-H_5-O_1$ is 163.4° at BLYP/6-31G and 170.3° at BLYP/6-31G*.

C. Electrostatic Potential Surfaces. The importance of electrostatic potential surfaces as a useful qualitative guide to study cation−π interactions has been pointed out by Dougherty and collaborators.[31] We present in Figures 4 and 5 different

TABLE 3: Structural Data Related to Hydrogen Bonding for the Cone Conformer and for the Protonated Cone Conformer of Calix[4]arene

	cone		cone-H^+		
	HFB/6-31G	BLYP/6-316	BLYP/6-31G*	BLYP/6-31G	BLYP/6-31G*
O_1-H_1	1.0252	1.0294	1.0074	1.0880	1.0687
H_1-O_2	1.7073	1.5880	1.6887	1.3903	1.4601
O_2-H_2	1.0252	1.0294	1.0074	1.0070	0.9981
H_2-O_3	1.7072	1.5878	1.6887	1.7340	1.7846
O_3-H_3	1.0252	1.0294	1.0074	0.9917	0.9848
H_3-O_4	1.7073	1.5880	1.6887		
H_4-O_3				1.7341	1.7860
O_4-H_4	1.0252	1.0294	1.0074	1.0070	0.99979
H_4-O_1	1.7073	1.5878	1.6887		
O_1-H_5				1.0877	1.0673
H_5-O_3					
H_5-O_4				1.3910	1.4638
$O_1-H_1-O_2$	161.4	161.1	165.1	163.4	170.5
$H_1-O_2-H_2$	104.9	105.0	103.2	110.9	107.9
$O_2-H_2-O_3$	161.4	161.1	165.1	158.0	159.4
$H_2-O_3-H_3$	104.9	105.1	103.2	116.8	115.7
$O_3-H_3-O_4$	161.4	161.1	165.1		
$H_3-O_4-H_4$	104.9	105.0	103.2		
$O_4-H_4-O_1$	161.4	161.1	165.1		
$H_4-O_1-H_1$	104.9	105.1	103.2	104.6	103.9
$H_1-O_1-H_5$				105.6	106.1
$O_3-H_4-O_4$				158.0	159.5
$O_4-H_5-O_1$				163.4	170.3

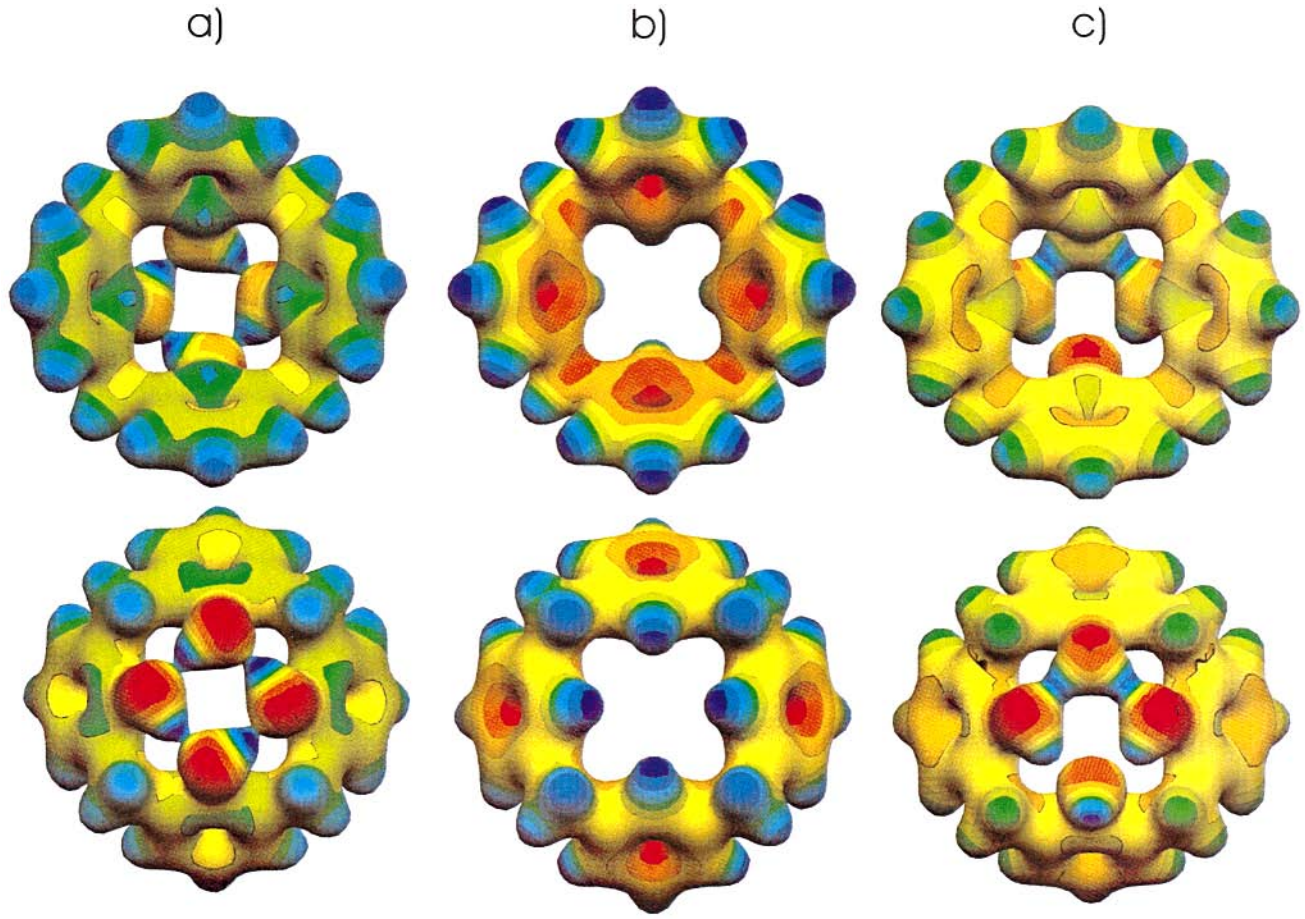

Figure 4. The electrostatic potential ϕ (in au) is represented over electronic isodensity ρ (in e Å^{-3}) surfaces of volume V_s (in Å^3). The color coding is the following: red corresponds to the minimum (negative) potential (ϕ_-) and blue to the maximum (positive) potential ϕ_+. All figures correspond to $\rho = 0.04$ e Å^{-3}. (a) cone calix[4]arene. $V_s = 148.2$, $\phi_- = -0.2053$, $\phi_+ = 0.1555$. (b) Tetra-O−H-depleted calix[4]arene. $V_s = 133.8$, $\phi_- = -0.1744$, $\phi_+ = 0.1102$. (c) protonated calix[4]arene. V_s −148.7, $\phi_- = -0.0803$, $\phi_+ = 0.3787$.

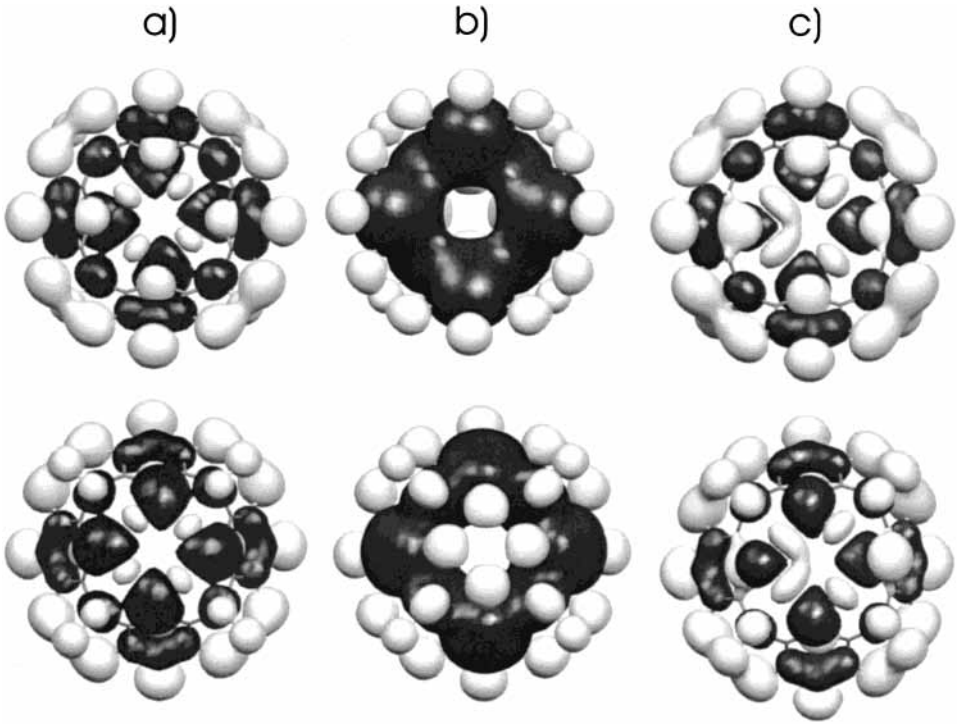

Figure 5. Electrostatic isopotential surfaces. The lower and upper limits of the electrostatic potential (in au) ($\phi_<$ and $\phi_>$ respectively) were determined over isoelectronic density surfaces of $\rho = 0.0004$ e Å^{-3}. (a) cone calix[4]arene: $\phi_< = -0.076$, $\phi_> = 0.030$. (b) Tetra-O−H-depleted calix[4]arene: $\phi_< = -0.084$, $\phi_> = 0.0235$. (c) Protonated calix[4]arene: $\phi_< = 0.033$; $\phi_> = 0.129$.

representations of the electrostatic potential for the cone calix[4]arene and protonated cone calix[4]arene. In order to analyze the O−H groups contribution to the electrostatic potential we are also reporting data on the tetra-O−H-depleted calix[4]arene in which H atoms replace O−H groups.

We observe that the convention for the colors is dependent on the lower and upper limits of the electrostatic potential. Consequently, for each system (cone, tetra-O−H-depleted cone and protonated cone) these limits should be consulted (see figure captions).

In Figure 4 the electrostatic potential is represented over an electronic isodensity surface of density $\rho = 0.04$ e Å^{-3}. On this surface, red regions are of relatively lower, or more negative electrostatic potential and blue regions correspond to higher or more positive electrostatic potential. From the images presented in Figure 4a, it is clear that the presence of the O−H groups in the lower rim of calix[4]arene contributes to define an extended region of strong and negative electrostatic potential. The formation of a cyclic hydrogen-bonded array that reflects the polarization of the O−H bonds is also illustrated. These features are useful to understand, at least from the electrostatic point of view, the well-known ability of calix[4]arenes to form complexes with cationic species.

For the tetra-O−H-depleted system (Figure 4b), the electrostatic potential is negative in the central region of the phenolic rings. This is related to the quadrupolar moment of benzene and helps to understand the importance of cation−π interactions in calix[4]arenes.[4,5]

The complexation of calix[4]arene with a proton (Figure 4c), modifies in a significant way the charge distribution and the electrostatic potential of the calix[4]arene system.

Figure 5 shows electrostatic isopotential surfaces. Details on the construction of these surfaces are given below. Initially, electronic isodensity surfaces with $\rho_e = 0.0004$ e Å^{-3} have been constructed for each system and the extrema of the electrostatic potential ($\phi_<$ and $\phi_>$) have been defined. Isopotential surfaces corresponding to these values are presented in Figure 5 where dark and light surfaces respectively correspond to $\phi_<$ and $\phi_>$.

For the tetra-O−H-depleted calix[4]arene, an extended isopotential surface corresponding to $\phi_<$ can be observed in the central region of the molecule. In the case of calix[4]arene, this region is localized in the lower rim of the molecule, suggesting that complexation with charged species can be favored. The change on the electrostatic potential induced by protonation of calix[4]arene is illustrated in Figure 5c. However, we observe that the shape of the surfaces and the limits of the potential are dependent on the electronic isodensity cutoff and the present construction of isopotential surfaces should be seen as a qualitative guideline to discuss complexation of calix[4]arene with charged species.

IV. Conclusions

This work reports density functional calculations for an important and complex molecule that is presently a model system in host−guest chemistry. We have compared our predictions for the conformational equilibrium with theoretical results based on force field and semiempirical methods. Our results suggest that the energy difference between 1,2-alternate and 1,3-alternate conformers of calix[4]arene is overestimated by force field calculations.

Density functional results for the structure of the cone calix[4]arene conformer are in very good agreement with experimental data.[29] However, some discrepancies are found when we compare force field predictions with experimental data.[29] This work also reports data on the structure and proton affinity of the calix[4]arene−H^+ complex. Unfortunately, we have no data from experimental or theoretical sources for comparison.

One of the conclusions of the present work concerns the analysis of the role played by calix[4]arene in host−guest chemistry made possible by visualization of electrostatic potential surfaces. Our results indicate that electrostatic potential surfaces can be relevant to understand, at least qualitatively, the ability of calix[*n*]arenes and derivatives to recognize neutral molecules and ions.

Acknowledgment. R. J. Bernardino gratefully acknowledges the support of the Portuguese Government through a Ph.D. Grant PRAXIS XXI/BD/4548/94. We are grateful to Dr. Paulo Couto for advise on the construction of the figures using the Molekel software.

References and Notes

(1) (a) Gutsche, C. D. *Calixarenes Revisited*; Stoddart, J. F., Ed. The Royal Society of Chemistry: Cambridge, 1998. (b) Pochini, A.; Ungaro, R. In *Comprehensive Supramolecular Chemistry*; Vögtle, F., Ed.; Pergamon: Elmsford, NY, 1996; Vol. 2, p 103.

(2) (a) Casnati, A. *Gazz. Chim. Ital.* **1997**, *127*, 637. (b) Ikeda, A.; Shinkai, S. *Chem. Rev.* **1997**, *97*, 1713. (c) Böhmer V. *Angew. Chem., Int. Ed. Engl.* **1995**, *34*, 717.

(3) Caldwell, J. W.; Kollman, P. A. *J. Am. Chem. Soc.* **1995**, *117*, 4177.

(4) Dougherty D. A. *Science* **1996**, *271*, 163.

(5) Ma, J. C.; Dougherty, D. A. *Chem. Rev.* **1997**, *97*, 1303.

(6) Lhoták P.; Shinkai, S. *J. Phys. Org. Chem.* **1997**, *10*, 273.

(7) Gutsche, C. D.; Bauer, L. J. *J. Am. Chem. Soc.* **1985**, *107*, 6052.

(8) Grootenhuis, P. D. J.; Kollman P. A.; Groenen, L. C.; Reinhoudt, D. N.; van Hummel, G. J.; Ugozzoli, F.; Andreetti, G. D. *J. Am. Chem. Soc.* **1990**, *112*, 4165.

(9) Royer, J.; Bayard, F.; Decoret, C. *J. Chim. Phys.* **1990**, *87*, 1695.

(10) Harada, T.; Rudzinski, J. M.; Osawa, E.; Shinkai, S. *Tetrahedron* **1993**, *49*, 5941.

(11) Lipkowitz, K. B.; Pearl, G. *J. Org. Chem.* **1993**, *58*, 6729.

(12) Harada, T.; Ohseto, F.; Shinkai, S. *Tetrahedron* **1994**, *50*, 13377.

(13) Harada, T.; S. Shinkai, S. *J. Chem. Soc., Perkin Trans.* **1995**, *2*, 2231.

(14) Fischer, S.; Grootenhuis, P. D. J.; Groenen, L. C.; van Hoornm W. P.; van Veggel, F. C. J. M.; Reinhoudt, D. N.; Karplus, M. *J. Am. Chem. Soc.* **1995**, *117*, 1611.

(15) Thondorf, I.; Brenn, J.; Brandt, W.; Böhmer, V. *Tetrahedron Lett.* **1995**, *36*, 6665.

(16) Bayard, F.; Fenet, B.; Lamartine, R.; Petit-Ramel, M.; Royer, J. *J. Chim. Phys.* **1995**, *92*, 13.

(17) Schätz, R.; Weber, C.; Schilling, G.; Oeser, T.; Huber-Patz, U.; Irngartinger, H.; von der Lieth, C. W.; Pipkorn, R. *Liebigs Ann.* **1995**, 1401.

(18) Brouyère, E.; Persoons, A.; Brédas, J. L. *J. Phys. Chem.* **1997**, *101*, 4142.

(19) Bernardino, R. J.; Costa Cabral, B. J.; Pereira, J. L. C. *J. Mol. Struct. (Theochem)* **1998**, *455*, 23.

(20) Becke, A. D. *Phys. Rev. A* **1988**, *38*, 3098.

(21) Becke, A. D. *J. Chem. Phys.* **1993**, *98*, 3098.

(22) Lee C.; Yang W.; Parr, R. G. *Phys. Rev. B* **1988**, *37*, 785.

(23) Frisch, M. J.; Trucks, G. W.; Schlegel, H. B.; Gill, P. M. W.; Johnson, B. G.; Robb, M. A.; Cheeseman, J. R.; Keith, T.; Peterson, G. A.; Montgomery, J.; Raghavachari, K.; Al-Laham, M. A.; Zakrzewski, V. G.; Ortiz, J. V.; Foresman, J. B.; Cioslowski, J.; Stefanov, B. B.; Nanayakkara, A.; Challacombe, M.; Peng, C. Y.; Ayala, P. Y.; Chen, W.; Wong, M. W.; Andres, J. L.; Repogle, E. S.; Gomperts, R.; Martin, R. L.; Fox, D. J.; Binkley, J. S.; DeFreees, D. J.; Baker, J.; Stewart, J. P.; Head-Gordon, M.; Gonzalez, C.; Pople, J. A. *Gaussian 94*; Gaussian, Inc.; Pittsburgh, PA.

(24) Dewar, M. J. S.; Zoebisch, E. G.; Healy, E. F. *J. Am. Chem. Soc.* **1985**, *107*, 3902.

(25) Stewart, J. J. P. *J. Comput. Chem.* **1989**, *10*, 209.

(26) Brooks, R.; Bruccoleri, R. E.; Olafson, B. D.; States, D. J.; Swaminathan, S.; Karplus, M. *J. Comput. Chem.* **1983**, *4*, 187.

(27) Allinger, N. L.; Yuh, Y. H.; Lii, J. H.; *J. Am. Chem. Soc.* **1989**, *111*, 8551.

(28) Flükiger, P. F. Molekel, *Molecular Visualization Software*; University of Geneva (http://igc.ethz.ch/molekel).

(29) Ungaro, R.; Pochini, A.; Andreetti, G. D.; Sangermano, V. *J. Chem. Soc., Perkin Trans.* **1984**, *2*, 1979.

(30) Wippf, G.; Lauterbach, M. *Supramol. Chem.* **1995**, *6*, 187.

(31) Mecozzi, S.; West, A. P., Jr.; D. A. Dougherty, D. A. *Proc. Natl. Acad. Sci. U.S.A.* **1996**, *93*, 10566.